***Word count: 6116**

Valuable rubidium extraction from potassium reduced seawater brine

Gayathri Naidu[a], Sanghyun Jeong[b], Youngkwon Choi[a], Min Hyung Song[b], Undram Oyunchuluun[a], Saravanamuthu Vigneswaran[a*]

[a] Faculty of Engineering, University of Technology Sydney (UTS), P.O. Box 123, Broadway, NSW 2007 Australia,

[b] Graduate School of Water Resources, Sungkyunkwan University (SKKU), 2066, Seobu-ro,
Jangan-gu, Suwon-si, Gyeonggi-do 16419, Republic of Korea,

*Corresponding author: Tel +61-2-9514-2641; Fax +61-2-9514-2633; Email: Saravanamuth.Vigneswaran@uts.edu.au

Abstract

Extraction of rubidium (Rb) which is an economically valuable metal from seawater reverse osmosis (SWRO) brine is beneficial. However, potassium (K) in SWRO brine hinders Rb extraction. Natural clinoptilolite zeolite in powder form was able to selectively remove K from SWRO brine (Langmuir maximum sorption, $Q_{max\ (cal.)} = 57.47 \pm 0.09$ mg/g). An integrated submerged membrane sorption reactor (SMSR) containing zeolite powder (300 g/L) achieved 65% K removal from SWRO brine. Periodic replacement of zeolite in SMSR, coupled with membrane backwashing with tap water was effective in maintaining a high K removal efficiency and a stable transmembrane pressure. Less than 5% Rb losses occurred along with K sorption, establishing the high K selectivity by zeolite in SWRO brine. The Rb sorption efficiency of polymer encapsulated potassium copper hexacyanoferrate (KCuFC(PAN)) sorbent from SWRO brine with reduced K contents, increased significantly from 18% to 83%.

Keywords: *Potassium; Potassium copper hexacyanoferrate; Rubidium; Seawater reverse osmosis brine; Sorption; Zeolite*

1. Introduction

Presently, potable water production by seawater reverse osmosis (SWRO) desalination (Fritzmann et al., 2007), environmental issues of SWRO brine discharge (Roberts et al., 2010), and economic interest in resource recovery (Jeppesen et al., 2009; Shahmansouri et al., 2015; Loganathan et al., 2017) have established that seawater and likewise SWRO brine are important and largely untapped sources of valuable elements.

Seawater contains vast mineral deposits that are rich in critical metals and valuable trace alkali elements (Loganathan et al., 2017). One such trace alkali metal with high economic potential (USD 14720.00/kg) is rubidium (Rb) (U.S. Geological Survey, 2016). Rb is used in specific fields such as fibre optic telecommunication and laser technology (Naidu et al., 2016a). A relatively large quantity of Rb is present in total seawater (156000 x 10^6 tonnes) compared to land mineral reserves (0.08 x 10^6 tonnes) U.S. Geological Survey, 2016). However, Rb is present at low concentrations (0.19 to 0.24 mg/L) with other dominant ions such as sodium (Na), calcium (Ca), magnesium (Mg) and potassium (K).

The capacity of potassium metal hexacyanoferrate sorbent, specifically potassium copper hexacyanoferrate (KCuFC) for selective Rb extraction/sorption under high saline conditions such as SWRO brine has been highlighted in a previous study (Naidu et al., 2016b). Nevertheless, Rb sorption efficiency of KCuFC is significantly reduced by 70 to 75% by the presence of K in SWRO brine (Naidu et al., 2016b).

In view of this, prior elimination of K in SWRO brine may effectively improve the Rb sorption efficiency of KCuFC. The application of natural zeolite (from various origins or different monocationic forms) for K sorption from seawater has been evaluated by previous studies (Cao et al., 2008; Hou et al., 2012). Although proven to be a favorable, the practical application of natural zeolite is still challenged due to its low K sorption capacity in seawater (14-20 mg/g), necessitating large column operation with high quantity of sorbent. Moreover, the fine-grain powdery condition of zeolite invariably causes bed clogging and decrease in filtration rates. A number of methods have been evaluated to overcome this limitation such as the application of magnetic zeolite (Cao et al., 2008) and potassium membrane (Yuan et al., 2012). Nevertheless, these methods tend to increase the overall extraction cost while the K sorption capacity from seawater remain low.

A submerged membrane sorption reactor (SMSR) which combines sorption and microfilter (MF) membrane process, is an integrated low energy system that offers an alternative solution to overcome the limitation of fixed bed column sorption. The SMSR system has been widely tested as a pretreatment for organic removal (Jeong et al., 2013; Johir et al., 2015). A few studies have evaluated the potential of SMSR for the sorption of selective ions (Reddad et al., 2003; Han et al., 2012). For instance, Reddad et al. (2003) used a dynamic MF reactor integrated with polysaccharide particles for the sorption of heavy metals, and indicated the technical feasibility of this approach as a low cost solution for treating polluted water. Similarly, Han et al. (2012) reported promising results on the removal of cesium (Cs) from tap water by an integrated sorption–MF process. These were attributed to continuous feed flow with suitable contact time that enabled to utilize the full capacity of sorbents in the reactor. Meanwhile the periodic renewal of new sorbents enabled to maintain high removal rates throughout the operation. Further, SMSR offers the flexibility to choose a suitable set of operating conditions (feed and permeate flow rate, hydraulic retention time and air flow) based on factors such as the sorption capacity and duration, reactor configuration and feed solution characteristics. An additional benefit of SMSR is the utilization of sorbent as fine powder instead of granular particles required in fixed bed columns. Sorbents as fine powder tend to achieve higher sorption capacity than as granular particles due to its higher surface area (Delkash et al., 2015).

Nonetheless, the usage of fine particles may increase the susceptible of membrane pore blocking and cake formation, resulting in transmembrane pressure increment. The approach of periodic renewal of new sorbents while withdrawing used sorbents has shown to be effective in preventing membrane pore blocking and cake formation, while providing fresh sorption sites for maintaining a continuous high sorption rate (Johir et al., 2015; Smith and Vigneswaran, 2009). Moreover, sorbents adhered on the MF membranes in SMSR can be removed with simple cleaning methods such as backwashing with tap water (Johir et al., 2015; Han et al., 2012). The potential of using SMSR for removing K from SWRO brine with zeolite has not been evaluated thus far.

Clinoptilolite is one of the most common naturally occurring zeolite (Smičiklas et al., 2007). Recently, very dense clinoptilolites have been identified which have been compressed by time and nature to form masses with essentially no macroporosity. One such of this clinoptilolite is produced by Castle Mountain, Australia (An et al., 2011). This natural zeolite do not have the fragile crystal grain boundaries found in synthetic zeolite analogues. Therefore, they have the mechanical robustness and have shown favourable performance as a natural zeolite membrane (An et al., 2011). The unique nature of this zeolite may enhance K sorption from SWRO brine.

It is well acknowledged that zeolite does exhibit selectivity for other monovalent ions including Cs (Smičiklas et al., 2007). Cs and Rb are both monovalent trace alkali metals with similar characteristics, implying that zeolite may simultaneously extract K with Rb from SWRO brine. As a result, Rb losses could occur prior to selective extraction with KCuFC sorbent. This factor must be evaluated in determining the suitability of zeolite for selective K removal from SWRO brine, prior to selective Rb extraction with KCuFC.

The objectives of this study, therefore, were to evaluate (i) natural zeolite’s capacity for K removal from SWRO brine; (ii) the suitability of using an integrated SMSR with powder form zeolite for removing K from SWRO brine, and (iii) comparison of Rb sorption efficiency of encapsulated KCuFC sorbent using K reduced SWRO brine compared to original SWRO brine.

2. Materials and methods

2.1. Solutions

Table 1. Characteristics of SWRO brine obtained from PSDP, Western Australia.

Parameters	**Unit**	**Value**
Total dissolved solids (TDS)	g/L	58.80 -58.93
pH		8.0 – 8.2
Dissolved organic carbon (DOC)	mg/L	1.29 -1.67
Major ion contents	mg/L	
Ca		789.30 -804.20
Mg		2390.50 - 2524.10
Na		23100.00 - 24800.00
K		790.20 – 810.10
Sr		15.42 – 16.11
Li		0.39 - 0.41
Rb		0.19 - 0.23

Stock solutions of K, Rb, Na, Sr, Ca and Mg were prepared by dissolving KCl, RbCl, NaCl, $SrCl_2$, $CaCl_2$ and $MgCl_2$ respectively in deionised (DI) water. All reagents were of analytical grade (Sigma-Aldrich) and were used without further purification. The initial and final ion concentration of the single solute solutions were determined by using Microwave Plasma - Atomic Emission Spectroscopy (MP-AES) (Agilent 4100, US) upon filtering the solution through a 1.2 µm glass fiber syringe filter.

The characteristics of SWRO brine obtained from Perth Seawater Desalination Plant (PSDP) in Western Australia are listed in **Table 1**. The ion concentrations of the SWRO brine were determined by inductively coupled plasma-mass spectrometry (ICP-MS, Agilent 7500, US). The total dissolved solids (TDS) and pH value were measured using an HQ40d portable pH meter (Hach, US). The dissolved organic contents (DOC) was measured with a TOC analyser (Shimadzu, Japan) upon filtration (0.45 µm Millipore filter).

2.2. Sorbent

2.2.1. Zeolite

The natural zeolite used in this study was purchased from Castle Mountain Zeolites (Quirindi, NSW, Australia). This zeolite is a clinoptilolite-rich mineral composed of clinoptilolite (~85 wt.%), mordenite (~15 wt.%) and trace amounts of quartz with a bulk density of 2.7 g/cm^3 (obtained from the supplier). The mineralogical composition (obtained from the supplier) is listed in **Table 2**.

Table 2. Chemical composition of zeolite.

Mineral content	**wt.%**
SiO_2	71.81
Al_2O_3	12.10
CaO	2.60
Na_2O	2.33
Fe_2O_3	1.14
K_2O	0.90
MgO	0.65
TiO_2	0.22
MnO	0.03
SrO	0.22
P_2O_5	<0.01
Loss on ignition	7.77

2.2.2. Polymer encapsulated potassium copper hexacyanoferrate, KCuFC(PAN)

Details on the preparation and characteristics of the laboratory-prepared polymer encapsulated KCuFC(PAN) is reported elsewhere (Naidu et al., 2016b).

2.3. Sorbent characterisation

2.3.1. Scanning electron microscopy with energy dispersive X-ray spectroscopy (SEM/EDX) analysis

The surface morphology and element contents of zeolite (before and after K sorption) were evaluated with scanning electron microscopy (SEM) coupled with energy dispersive X-ray spectroscopy (EDX) operated at 15 kV (Zeiss Supra 55VP Field Emission).

2.3.2. Powder X-ray diffraction analysis (XRD)

XRD data on zeolite (before and after K sorption) were collected on a Siemens D5000 diffractometer operating with CuK alpha-radiation and a rotating sample stage. The samples were scanned at room temperature in the 2Θ angular range of 20–110º.

2.3.3. pH and zeta potential

The effect of pH on K sorption at equilibrium condition was investigated at acidic and basic conditions. For this purpose, 0.6 g/L zeolite was suspended in glass flasks containing 100 mL of 790 ± 5 mg K/L solution in the pH range of 3 to 11. These flasks were agitated for 24 h in a flat shaker (120 rpm speed; 24 ± 1 ºC). The initial pH values were adjusted using NaOH and HCl solutions. The initial pH ($pH_{initial}$) and equilibrium pH (pH_{eq}) of the solutions were measured using an HQ40d portable pH meter (Hach).

Zeta potential measurement was carried out to determine the sorbent surface charge. For this purpose, 0.6 g/L zeolite was suspended in glass flasks containing 100 ml of 10^{-3} M KCL in the pH range of 3 to 11. The suspensions were agitated for 24 h in a flat shaker. Zeta values were measured with a Zetasizer nano instrument (Nano ZS Zen3600, Malvern, UK) upon recording the pH_{eq} of the solutions.

2.4. Sorption experiments

All batch sorption experiments with zeolite were conducted with K solution at a concentration of 790 ± 5 mg K/L, corresponding to the K concentration in SWRO brine (**Table 1**). Experiments were performed in a set of glass flasks containing zeolite with 100 mL of solutions. The flasks were agitated in a flat shaker at a shaking speed of 120 rpm at room temperature (24 ± 1 ^{o}C). The solution pH was initially adjusted to a predetermined value (based on the pH evaluation test) and re-adjusted to the same value after 4 h and 8 h with HCl or NaOH solutions, to ensure a constant pH was maintained throughout the sorption duration. Experiments were duplicated and the average values were recorded for data analysis. The difference between the duplicate values were within ±2%.

2.4.1. Sorption isotherm

Batch equilibrium sorption experiments were conducted at different doses of zeolite ranging from 0.2 to 400 g/L. The K sorption amount at equilibrium, q_e (mg/g), was calculated based on the difference between K concentration in the initial C_0 and equilibrium C_e (mg/L) solution, per volume of solution, V (L) and sorbent mass, M (g) (Naidu et al., 2016b). The sorption data were evaluated using Langmuir isotherm based on previous studies on K sorption with zeolite which showed good isotherm model fitting (Guo et al., 2008; Hor et al., 2016; Guo et al., 2017).

2.4.2. Sorption kinetics

Sacrificial batch sorption kinetics were conducted with zeolite dose of 0.6 g/L (selected based on isotherm results). The suspensions were agitated for time intervals ranging from 10 min to 24 h. The ion concentrations of the solutions collected at these different time intervals were measured. The sorption amount (q_t) at time t was calculated and evaluated using pseudo-second order (PSO) kinetic model. This model was chosen based on its good fitting of K sorption with zeolite from previous studies (Guo et al., 2008; Hor et al., 2016; Guo et al., 2017).

2.5. Influence of co-existing SWRO brine ions on K sorption

The selectivity of zeolite towards K in the presence of major inorganic ions in SWRO brine (Na, Ca, Mg and Sr) was evaluated in this study. Further, the possibility of co-sorption of Rb during K sorption was evaluated. All experiments were conducted with an initial K concentration of 790 ± 5 mg K/L and zeolite dose of 1.2 g/L while the competitor ion concentrations were set at a range of concentration emulating SWRO brine as listed in **Table 1**. The pH value of the solutions were maintained at a predetermined value (based on the pH evaluation test).

2.6. Submerged membrane sorption reactor (SMSR)

2.6.1. Experimental set-up

The SMSR (**Fig. 1**) consist of a reactor containing SWRO brine maintained at a constant volume of 4 L with a submerged hollow fiber microfilter (MF) membrane (Cleanfil®-S, Kolon membrane) (effective membrane surface area of 0.08 m^2). The MF membrane was made of three materials (Polysulfone, Polyethersulfone, Polyvinlidene Fluoride) with a nominal pore size of 0.1 µm, inner and outer diameter of 1.1 mm and 2.1 mm respectively.

For the SMSR operation, a predetermined amount of zeolite was initially dosed into the reactor followed by periodic sorbent replacement (approximately 25% of the initial predetermined sorbent) to maintain a 60% K removal from SWRO brine. Periodic zeolite renewal was carried out by withdrawing a measured volume of suspension, filtering the used zeolite, and replacing fresh zeolite in equivalent amount to the used sorbent withdrawn. The effluent samples were collected at regular time intervals to analyse the ion concentrations. The SMSR operation was carried out for a duration of 7 h.

Air was supplied from the bottom of the reactor using an external aerator at a rate of 3.5 L/min to keep the zeolite in suspension. Effluent/permeate was channelled out using a peristaltic pump at a constant flux of 8.0 L/m^2 h (LMH), maintaining a hydraulic retention time (HRT) of 6.3 h. This was based on previous zeolite K sorption studies which indicated achieving maximum sorption by a duration of 4 - 6 h (Guo et al., 2008; Guo et al., 2017).

The transmembrane pressure (TMP) was automatically measured using a pressure transducer (PTX 1400 Druck Industrial Pressure Sensor, Druck Limited, UK) installed between the membrane and permeate peristaltic pump.

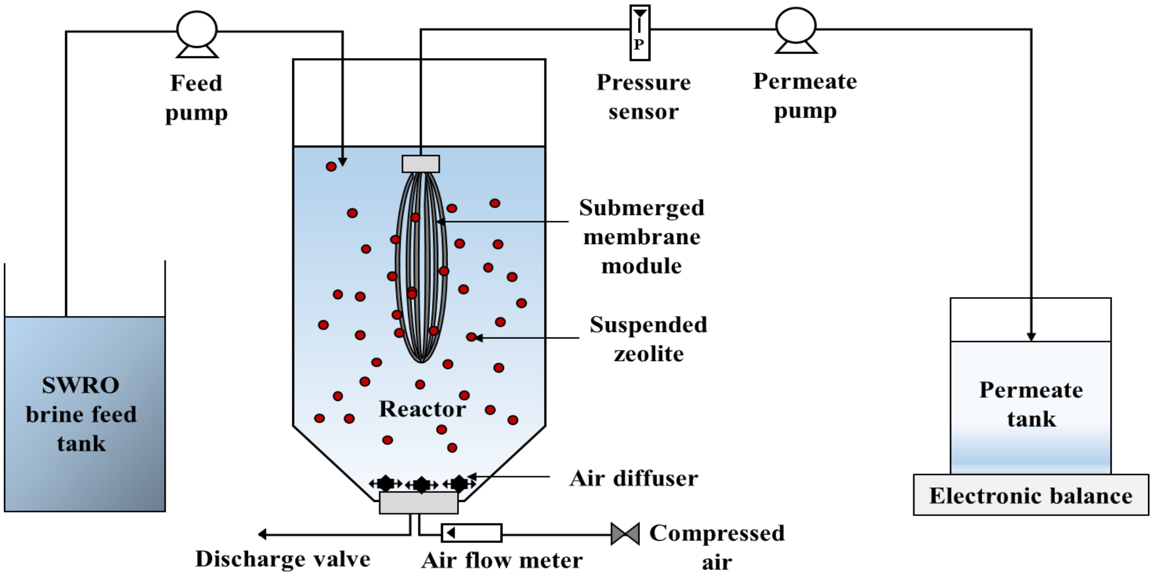

Fig. 1. A schematic diagram of submerged membrane sorption reactor (SMSR) system.

2.6.2. Membrane cleaning

Periodic membrane backwashing with tap water at a high flow rate of 5 L/h for 5 min was carried out every 2 h throughout the SMSR operation. At the end of the SMSR operation, a portion of the used MF membrane was soaked in a beaker containing 0.1% NaOCl for 4 h. The beaker was kept in suspension at a speed of 40 rpm. Membrane autopsy (SEM/EDX) of the virgin, used (tap water washed) and chemically cleaned membranes were carried out per the procedure described in **Section 2.3.1**.

2.7. Rb sorption by KCuFC(PAN) with SWRO brine (reduced K contents)

The performance of KCuFC(PAN) on Rb sorption using SWRO brine with reduced K contents as well as original SWRO brine was evaluated in terms of sorption isotherm using the same procedure reported in **Section 2.4.1.**

3. Results and discussion

3.1. Characteristics of zeolite

3.1.1. SEM-EDX analysis

The SEM images showed similar zeolite appearance before and after K sorption (**Fig. S1)**. The heterogeneous condition of natural zeolite was attributed to the combination of different zeolite phases with other crystalline and amorphous materials (Elaiopoulos et al., 2010). The EDX emission pattern revealed the presence of O, Si, Al, K, Na, Mg, Ca and Fe peaks in the zeolite structure (**Fig. S1**). O, Si and Al are the major elements in zeolite, with relatively low presence of Na, Ca, Mg, K and Fe (< 2% atomic ratio). This was in line with the sorbent chemical composition listed in **Table 2**. Both the EDX and chemical composition showed a good match of Si/Al molar ratio at 5.0 and above. Similar values were reported in previous studies using natural zeolite (An et al., 2011; Elaiopoulos et al., 2010; Camacho et al., 2011). A high Si/Al ratio indicate a high negative charge of the zeolite structure, which is beneficial in increasing the sorbent surface affinity towards positively charged ions.

Upon K sorption, a higher K peak intensity was observed in the EDX spectra with a reduction of Na and Ca peak intensity, suggesting the likely exchange of K with Na and Ca.

3.1.2. Powder X-ray diffraction (XRD) analysis

The XRD composition of the original zeolite was consistent with other studies, matching the structure of natural clinoptilolite zeolite (Wang et al., 2007; Guo et al., 2016). The same diffraction peaks were observed for both the original and K sorbed zeolite, confirming no changes of crystal structure occurred upon K sorption by zeolite (**Fig. S2**).

3.2. Influence of pH on K sorption

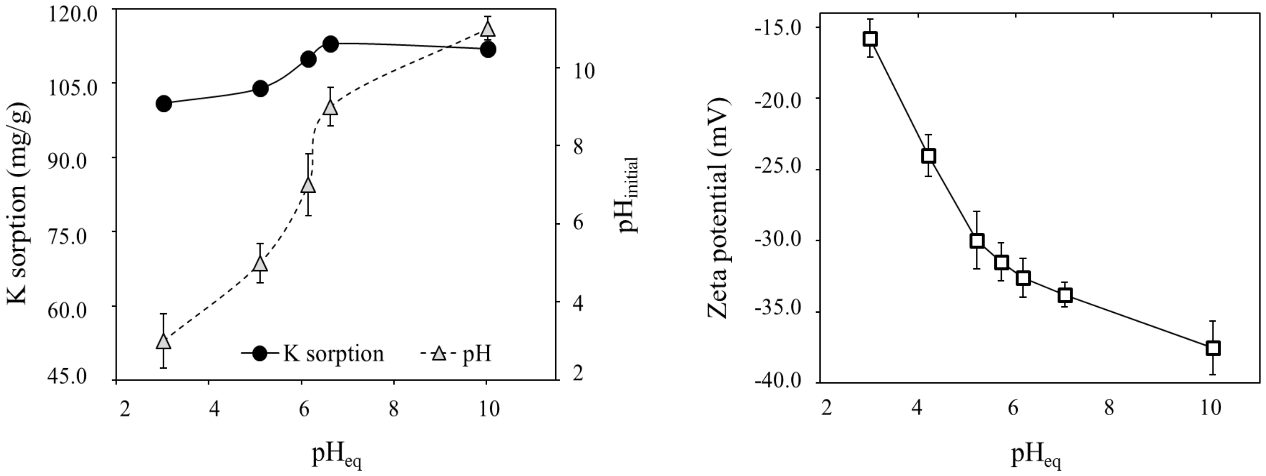

(a) **(b)**

Fig. 2. Influence of pH on zeolite (dose = 0.6 g/L) in terms of **(a)** K sorption and pH variation (C_o = 790 ± 5 mg K/L) **(b)** zeta potential with 10^{-3} M KCl.

The equilibrium pH (pH_{eq}) showed an increase of initial pH values in acidic conditions and a decrease of initial pH values in alkaline conditions (**Fig. 2a**). This trend indicated the tendency of zeolite to neutralize the solution acting as a proton acceptor or as a proton donor depending on the pH. K sorption by zeolite was minimally influenced by the change of pH values, especially above pH_{eq} of 6 (**Fig. 2a**). Similar observations were made by other studies on K and Cs sorption with zeolite (Smičiklas et al., 2007; Guo et al., 2016). The slightly lower K sorption at low pH (below pH_{eq} 6) could be due to the competition of H with K for sorption sites in highly acidic solution. The minimal K sorption reduction observed above pH_{eq} 6 could be associated to the high negative surface charge of zeolite at higher pH as indicated by the zeta potential trend (**Fig. 2b**). The zeolite surface zeta potential of -17 to -24 mV at pH_{eq} below 6 increased to higher negative values (-34 to -39 mV) at pH_{eq} above 6. Similarly, Englert and Rubio (2005) showed a trend of more negative zeta potential at higher solution pH for natural zeolite. Increased negative surface of zeolite above pH_{eq} of 6 would increase the sorption affinity towards positively charged ions such as K by electrostatic sorption (outer sphere complexation).

Based on the zeta potential and K sorption trend at different pH, all further experiments were carried out at a constant pH of 8.0 ± 0.5, corresponding to the pH of SWRO brine (**Table 1)**.

3.3. Equilibrium isotherm and kinetics with pure K solution

Table 3 The parameters of Langmuir isotherm and PSO kinetics model for K sorption by zeolite with K solution and SWRO brine.

Model type	Parameter	Solution type	
		K solution	SWRO brine
Langmuir	Experimental $Q_{max(exp.)}$ (mg/g)	208.53 ± 0.13	51.50 ± 0.11
	Calculated $Q_{max(cal.)}$ (mg/g)	217.68 ± 0.17	57.47 ± 0.09
	K_L (L/mg)	0.02 ± 0.01	0.02 ± 0.01
	R^2	0.97	0.97
Pseudo second order (PSO)	Experimental $q_{e(exp.)}$ (mg/g)	114.67 ± 0.10	44.51 ± 0.09
	Calculated $q_{e(cal.)}$ (mg/g)	122.32 ± 0.13	46.72 ± 0.05
	k_2 x 10^{-4} (g/mg min)	0.48 ± 0.03	3.67 ± 0.02
	R^2	0.98	0.97

K sorption by zeolite fitted well to Langmuir model (R^2 = 0.97), achieving a $Q_{max(cal.)}$ of 217.68 ± 0.17 mg/g (**Fig. 3a**, **Table 3**). Similarly, Cao et al. (2008) reported a K sorption of 245.1 mg/g with zeolite.

K sorption increased with time achieving a maximum sorption within 8 h with 0.6 g/L of zeolite (**Fig. 3b**). The data fitted well to the PSO model (R^2 = 0.98), with a derived $q_{e(cal.)}$ of 122.32 ± 0.13 mg/g, matching well with the experimental $q_{e(exp.)}$ of 114.67 ± 0.10 mg/g (**Fig. 3b, Table 3**). In correspondence with K sorption, Na and Ca releases were detected throughout the entire sorption duration (**Fig. S3**). Previous studies have indicated that Na and Ca are the major cations involved in the zeolite exchange process (Abusafa and Yücel, 2002). At the same time, the presence of Si was detected in the solution. Nevertheless, similar Si concentration over the sorption duration indicated that Si did not participate in the exchange mechanisms and was merely residues released from the zeolite structure. Neligible presence of Al, Fe and Mg ions were detected over time

3.4. Equilibrium isotherm and kinetics with SWRO brine

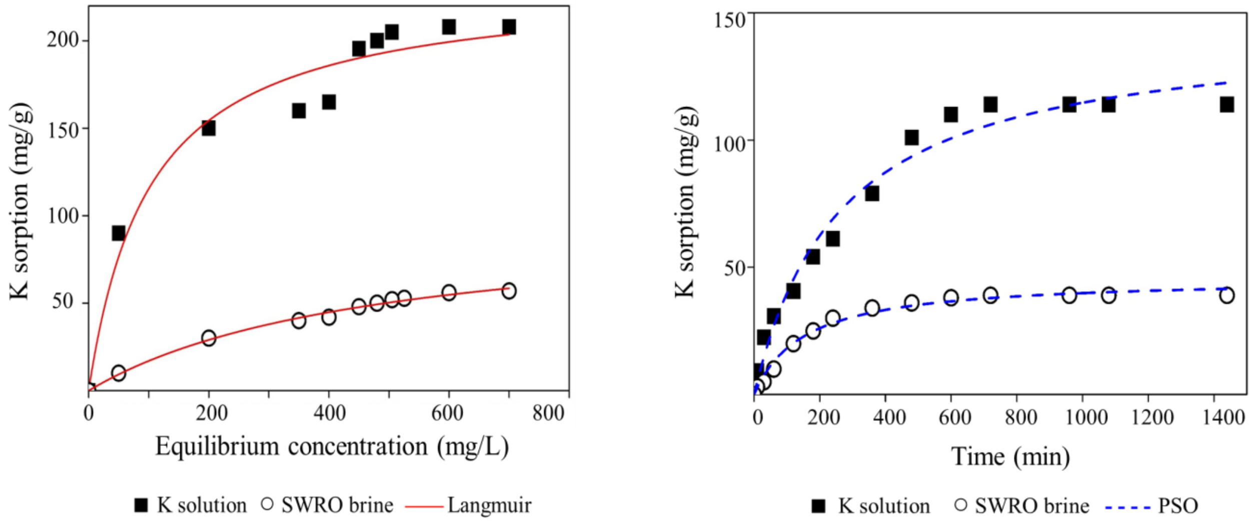

(a) **(b)**

Fig. 3. K sorption by zeolite with pure K solution and SWRO brine **(a)** equilibrium Langmuir isotherm model fit **(b)** PSO kinetics model fit (C_o= 790 ± 5 mg K/L; pH_{eq} = 8.0 ± 0.5; kinetic zeolite dose = 0.6 g/L).

In SWRO brine, zeolite exhibited a maximum K sorption capacity with an experimental value, $Q_{max(exp.)}$ of 51.50 ± 0.06 mg/g. The theoretical $Q_{max(cal.)}$ of 57.47 ± 0.08 mg/g obtained by Langmuir model (R^2 = 0.97) was in good agreement with the actual experimental value (**Fig. 3a, Table 3**). At a dose of 0.6 g/L zeolite, maximum K sorption in SWRO brine was achieved within a duration of 6 to 7 h, with a derived $q_{e(cal.)}$ of 46.72 ± 0.02 mg/g (**Fig. 3b, Table 3**). The 75% lower K sorption in SWRO brine compared to pure K solution indicated that the presence of other ions in SWRO brine influenced the zeolite performance. A detail evaluation on coexisting ion competition is discussed in **Section 3.4.1**.

Although the K sorption capacity of natural zeolite in powder form was reduced considerably in SWRO brine compared to pure K solution, it still showed considerably superior capacity in comparison to previous studies that indicated K sorption capacity from seawater in the range of 14 to 20 mg/g (Cao et al., 2008; Hou et al., 2012).

3.4.1. Influence of co-existing SWRO brine ions on K sorption

K solutions with Na, Ca, Mg, Sr and Rb, spiked at molar concentrations representing SWRO brine was used to evaluate the influence of co-existing SWRO brine ions on K sorption by zeolite. The presence of these ions reduced K sorption capacity of zeolite in the order of Ca > Mg > Na while negligible changes were observed with Rb and Sr (**Fig. 4a**). The influence of these ions on K sorption was associated to factors such as ionic radius, zeolite structure, ion charge, and ion concentration (Mimura and Kanno, 1985; Abusafa and Yücel, 2002).

In the presence of high Na (23-24 g/L), K sorption reduced by 33% while a 5% of Na sorption occurred. This indicated that Na and K competed for zeolite surface sorption sites. Nevertheless, due to the smaller ionic radius of K (**Table 4**) (Lehto et al., 1992; Smičiklas et al, 2007; Qing et al, 2015), it tend to adsorb more easily on the sites of tunnel-like structure of zeolite, compared to Na. Meanwhile, divalent Mg (2.4 -2.5 g/L), having higher ion charge compared to monovalent K, reduced the ion exchangeability between K and Ca. As a result, K sorption reduced by 46%, while 4% sorption of Mg occurred. The presence of Ca (0.78 – 0.80 g/L) reduced the exchange affinity between Ca in the zeolite structure with K, attributed to ion saturation, resulting in a 65% K sorption reduction.

Generally, zeolite exhibit a selectivity in the order of Cs > Rb > K > Na > Sr > Ca >Mg (Abusafa and Yücel, 2002) based on the ionic radius size as shown in **Table 4**. This implied the high affinity of zeolite towards Rb and Sr, which are present in SWRO brine (**Table 1**). Nevertheless, the presence of Sr (9.5-10.5 mg Sr/L) and Rb (0.20-0.23 mg Rb/L), in concentrations representing SWRO brine, did not significantly affect K sorption and neither were these ions sorbed by zeolite (**Fig. 4a**). The minimal influence of these ions could be related to their low concentrations compared to 750 - 780 mg K/L in SWRO brine. Likewise, as predicted, in actual SWRO brine, a combination of all the major ions led to 70-75% K sorption reduction with a 2% Na sorption. During the selective K sorption in SWRO brine by zeolite, Rb sorption/losses did not occur. It is also worth mentioning that the low DOC contents in SWRO brine (**Table 1**) would not have a significant effect on zeolite performance towards K sorption, as reported by Mitrogiannis et al. (2017).

3.4.2. K removal efficiency in SWRO brine

In SRWO brine, higher K sorption/removal efficiency in SWRO brine was achieved with increased zeolite doses (**Fig. 4b)**. Higher sorbent doses increased the availability of exchangeable sites enabling to achieve higher removal efficiencies. A total of 72% K sorption was achieved with 400 g/L zeolite. This was accompanied by 20% Na sorption. At high zeolite doses (> 200 g/L), a 2-5% Rb sorption occurred, while at low doses (< 200 g/L), minimal Rb losses occurred. This could explain the observation in **Section 3.4.1** indicating negligible Rb losses, in which, the test was carried out at low zeolite dose of 1.2 g/L. Nevertheless, even at high zeolite doses, Rb losses (2-5%) were considerably minimal.

Table 4. Hydrated and unhydrated ionic radius of major elements and trace alkali metal in SWRO brine (Letho et al., 1992; Smičiklas et al., 2007; Qing et al., 2017).

Elements	Hydrated ionic radius, Å	Unhydrated ionic radius, Å
Cs	2.26 - 2.28	1.68-1.69
Rb	2.28 -2.29	1.48-1.53
K	2.32 - 3.31	1.33-1.37

Na	2.76 - 3.60	0.95 -0.12
Sr	3.80 - 4.12	1.00- 1.13
Ca	4.10 - 4.13	1.00 -1.12
Mg	4.28 -4.30	0.72 - 0.81

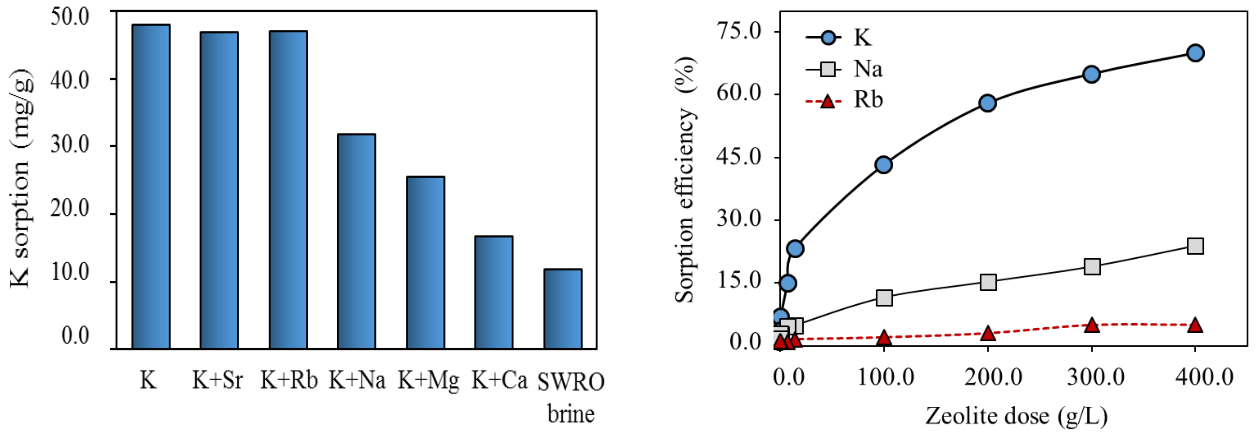

(a) **(b)**

Fig. 4. Performance of zeolite in SWRO brine **(a)** influence of co-existing ions on K sorption/removal (zeolite dose =1.2 g/L) **(b)** sorption/removal efficiency of K, Na and Rb as a function of zeolite dose.

3.5. Submerged membrane sorption reactor (SMSR) with SWRO brine

3.5.1. K removal

SMSR was operated with SWRO brine and zeolite at a dose of 300 g/L for a duration of 7 h. In view of the high amount of zeolite dose required, the SMSR operation was carried out with periodic sorbent replacement. The approach provided the flexibility of withdrawing 25% of the used zeolite while replacing similar amount of new zeolite for K sorption. This was beneficial in maintaining the same zeolite dose throughout the operation duration, while providing fresh surface sites for K sorption. The SMSR operation enabled to maintain 65% K sorption/removal in SWRO brine (**Fig.**

5a) throughout the operation duration of 7 h, accompanied by 15% removal of Na and 2-5% Rb removal.

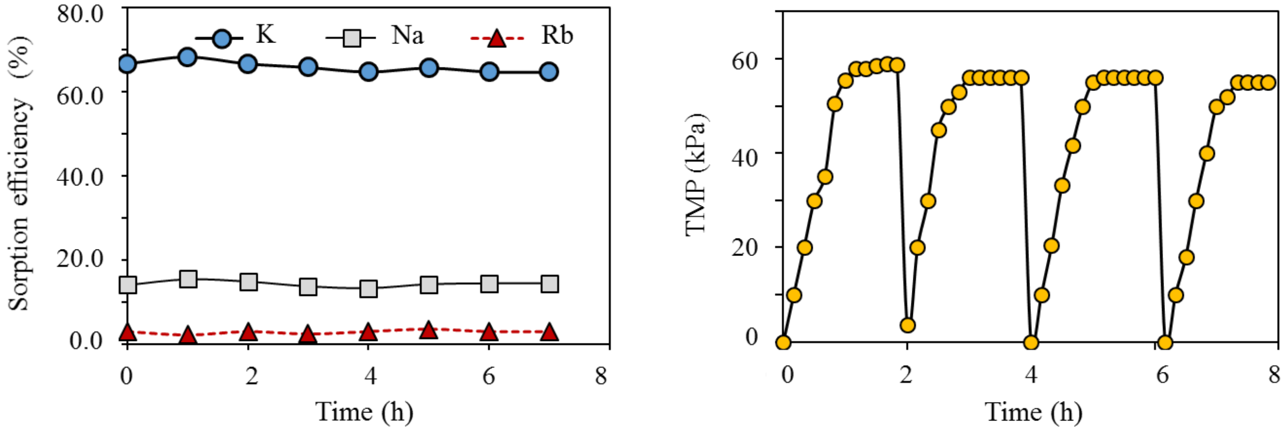

(a) **(b)**

Fig. 5. SMSR operation with SWRO brine as a function of time **(a)** sorption/removal efficiency of K, Na and Rb **(b)** TMP trend (zeolite dose = 300 g/L; permeate flux = 8.0±0.5 LMH).

3.5.2. Trans membrane pressure (TMP) development

The TMP increased to 60 kPa after 2 h of SMSR operation (**Fig. 5b**). The membrane was covered with a thick layer of zeolite, which was most likely the main cause of the high TMP build-up. As a mitigation measure, intermittent backwashing of the membrane was carried out every 2 h of the SMSR operation with tap water at a flow rate of 5 L/h for 5 min. The zeolite adhered onto the membrane was easily removed by this simple backwashing with tap water, thereby enabling to restore the TMP to its initial level and maintain the TMP at 60 kPa throughout the SMSR operation (**Fig. 5b**).

3.5.3. Membrane analysis

The cross section and surface of the virgin membrane, used membrane (with tap water backwashing) and chemically cleaned membrane (0.1% NaOCl) were analysed with SEM-EDX (**Fig. S4**). The

SEM images showed similar appearance for all membranes while the presence of tiny particles were observed on the used membrane surface (**Fig. S4b**). The EDX element analysis of the used membrane cross-section revealed the presence of Na, Ca, Mg, S and Cl, which are dominant elements present in SWRO brine. Meanwhile, on the used membrane surface, apart from these elements, traces of Si, K and Al were also detected. This was likely attributed to zeolite, which could be related to the particles observed on the used membrane surface. The presence of zeolite on the surface of the used membrane and not on the cross section established that zeolite did not block the membrane pores and predominately adhered on the membrane surface. This explains the effectiveness of simple tap water backwashing in removing most of the zeolite layer during the SMSR operation. The chemical cleaned membrane (**Fig. S4c**) showed similar characteristics to the virgin membrane (**Fig. S4a**), with no traces of particles. This established the capacity of the membrane to be restored to its initial condition with simple chemical cleaning.

3.6. Rb sorption from K reduced SWRO brine by KCuFC(PAN)

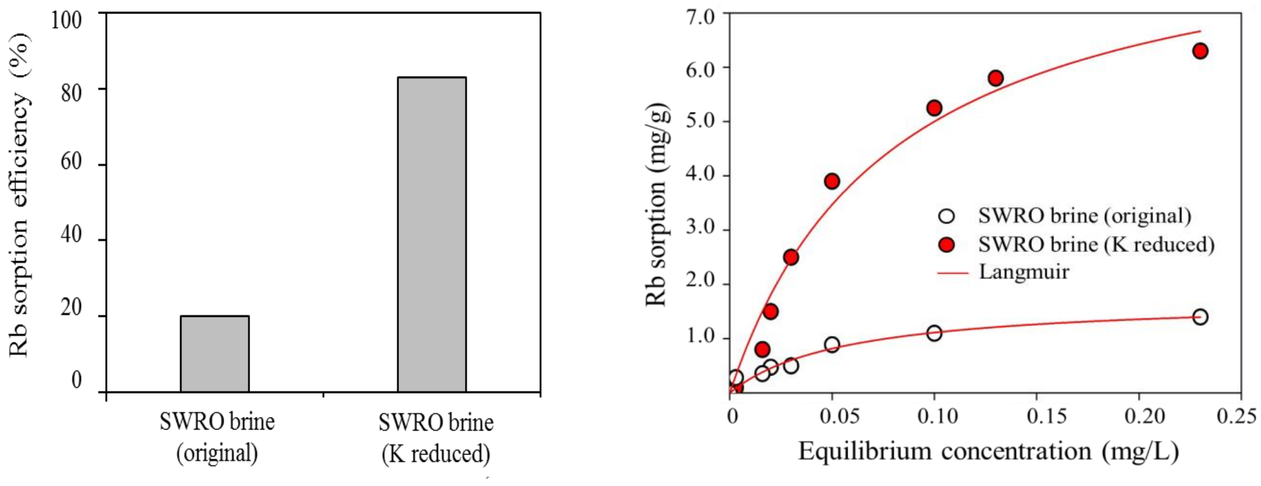

(a) **(b)**

Fig. 6. Comparison of Rb sorption by KCuFC(PAN) with original SWRO brine and K reduced SWRO brine **(a)** sorption efficiency at same sorbent dose (0.4 g/L) **(b)** equilibrium Langmuir isotherm model fit ($pH_{eq} = 8.0 \pm 0.5$).

KCuFC(PAN) exhibited a significantly better Rb sorption capacity with K reduced SWRO brine compared to the original SWRO brine. At the same KCuFC(PAN) dose (0.4 g/L), a 83% Rb sorption from K reduced SWRO brine was achieved compared to 18% Rb sorption with the original SWRO brine **(Fig. 6a)**. A maximum Rb sorption, Langmuir $Q_{max(cal.)}$ of 7.83 ± 0.02 mg/g was achieved with K reduced SWRO brine **(Fig. 6b)**. Meanwhile, a maximum Rb sorption, Langmuir $Q_{max(cal.)}$ of 1.81 ± 0.04 mg/g was achieved with K reduced SWRO brine. The results established the positive benefit of reducing K contents in SWRO brine for enhancing the performance of KCuFC(APN) for efficient Rb selectivity.

4. Conclusions

In SWRO brine, the K sorption capacity by natural clinoptilolite zeolite (powder form) reduced by 75% compared to pure K solution. The presence of Na, Mg and Ca in SWRO brine reduced the K sorption efficiency of zeolite. An integrated SMSR system with zeolite (dose of 300 g/L) achieved 65% K removal for 7 h. Membrane backwashing with tap water every 2 h and zeolite replacement enabled to maintain stable K removal efficiency and TMP. Selective Rb sorption efficiency by KCuFC(PAN) sorbent was significantly increased to 83% with K reduced SWRO brine, achieving a $Q_{max(cal.)}$ of 7.83 ± 0.02 mg/g.

Acknowledgements

This work was funded by Australian Research Council Discovery Research Grant (DP150101377). We also acknowledge the team from Perth Seawater Desalination Plant (Robert Vollprecht and Ushi Jismi) for the provision of seawater reverse osmosis brine.

References

Abusafa, A., Yücel, H., 2002. Removal of ^{137}Cs from aqueous solutions using different cationic forms of a natural zeolite : clinoptilolite. Sep. Purif. Technol. 28, 103–116.

An, W., Swenson, P., Wu, L., Waller, T., Ku, A., Kuznicki, S.M., 2011. Selective separation of hydrogen from C_1/C_2 hydrocarbons and CO_2 through dense natural zeolite membranes. J. Memb. Sci. 369, 414–419

Camacho, L.M., Parra, R.R., Deng, S., 2011. Arsenic removal from groundwater by MnO_2-modified natural clinoptilolite zeolite: Effects of pH and initial feed concentration. J. Hazard. Mater. 189, 286–293.

Cao, J., Liu, X.W., Fu, R., Tan, Z.Y, 2008. Magnetic P zeolites: Synthesis, characterization and the behavior in potassium extraction from seawater. Sep. Purif. Technol. 63, 92–100.

Delkash, M., Ebrazi Bakhshayesh, B., Kazemian, H., 2015. Using zeolitic adsorbents to cleanup special wastewater streams: A review. Microporous Mesoporous Mater. 214, 224–241.

Elaiopoulos, K., Perraki, T., Grigoropoulou, E., 2010. Monitoring the effect of hydrothermal treatments on the structure of a natural zeolite through a combined XRD, FTIR, XRF, SEM and N2-porosimetry analysis. Micro. Meso. Mater. 134, 29–43.

Englert, A.H., Rubio, J., 2005. Characterization and environmental application of a Chilean natural zeolite. Int. J. Miner. Process. 75, 21–29.

Fritzmann, C., Löwenberg, J., Wintgens, T., Melin, T., 2007. State-of-the-art of reverse osmosis desalination. Desalination 216, 1-76.

Guo, H., Peng, C.S., Kou, C.J., Jiang, J.Y., Zhang, F., Yuan, H.T., 2017. Adsorption mechanism of recovering potassium from seawater by modified-clinoptilolite using microwave. J. Water Reuse Desalin.

Guo, X., Zeng, L., Li, X., Park, H.S., 2008. Ammonium and potassium removal for anaerobically digested wastewater using natural clinoptilolite followed by membrane pretreatment. J. Hazard. Mater. 151, 125–133.

Guo, X.F., Ji, Z.Y., Yuan, J.S., Zhao, Y.Y., Liu, J., 2016. Recovery of K^+ from concentrates from brackish and seawater desalination with modified clinoptilolite. Desalin. Water Treat. 57, 6829–6837.

Han, F., Zhang, G.H., Gu, P., 2012. Removal of cesium from simulated liquid waste with countercurrent two-stage adsorption followed by microfiltration. J. Hazard. Mater. 225–226, 107–113.

Hor, K.Y., Chee, J.M.C., Chong, M.N., Jin, B., Saint, C., Poh, P.E., Aryal, R., 2016. Evaluation of physicochemical methods in enhancing the adsorption performance of natural zeolite as low-cost adsorbent of methylene blue dye from wastewater. J. Clean. Prod. 118, 197–209.

Hou, J., Yuan, J., Shang, R., 2012. Synthesis and characterization of zeolite W and its ion-exchange properties to K^+ in seawater. Powder Technol. 226, 222–224.

Jeong, S., Naidu, G., Vigneswaran, S., 2013. Submerged membrane adsorption bioreactor as a pretreatment in seawater desalination for biofouling control. Bioresour. Technol. 141, 57–64.

Jeppesen, T., Shu, L., Keir, G., Jegatheesan, V., 2009. Metal recovery from reverse osmosis concentrate. J. Clean. Prod. 17, 703–707.

Johir, M.A.H., Shim, W.G., Pradhan, M., Vigneswaran, S., Kandasamy, J., 2015. Benefit of adding adsorbent in submerged membrane microfiltration treatment of wastewater. Desalin. Water Treat. 3994, 1–11.

Lehto, J., Paajanen, R., Harjula, R., 1992. Selectivity of potassium cobalt hexacyanoferrate (II) for alkali and alkaline earth metal ions, J. Radioanal. Nucl. Chem. 164, 39–46.

Loganathan, P., Naidu, G., Vigneswaran, S., 2017. Mining valuable minerals from seawater: a critical review. Environ. Sci. Water Res. Technol. 3, 37–53.

Mimura, H., Kanno, T., 1985. Distribution and Fixation of Cesium and Strontium in Zeolite A and Chabazite. J. Nucl. Sci. Technol. 22, 284–291.

Mitrogiannis, D., Psychoyou, M., Baziotis, I., Inglezakis, V.J., Koukouzas, N., Tsoukalas, N., Palles, D., Kamitsos, E., Oikonomou, G., Markou, G., 2017. Removal of phosphate from aqueous solutions by adsorption onto $Ca(OH)_2$ treated natural clinoptilolite, Chem. Eng. J. 320, 510–522.

Naidu, G., Loganathan, P., Jeong, S., Johir, M.A.H., To, V.H.P., Kandasamy, J., Vigneswaran, S., 2016b. Rubidium extraction using an organic polymer encapsulated potassium copper hexacyanoferrate sorbent. Chem. Eng. J. 306, 31–42.

Naidu, G., Nur, T., Loganathan, P., Kandasamy, J., Vigneswaran, S., 2016a. Selective sorption of rubidium by potassium cobalt hexacyanoferrate. Sep. Purif. Technol. 163, 238–246.

Qing, Y.H., Li, J., Kang, B., Chang, S.Q., Dai, Y.D., Long, Q., Yuan, C., 2015. Selective sorption mechanism of Cs^+ on potassium nickel hexacyanoferrate(II) compounds. J. Radioanal. Nucl. Chem. 304, 527–533.

Reddad, Z., Gérente, C., Andrès, Y., Thibault, J.F., Le Cloirec, P., 2003. Cadmium and lead adsorption by a natural polysaccharide in MF membrane reactor: Experimental analysis and modelling. Water Res. 37, 3983–3991.

Roberts, D.A., Johnston, E.L., Knott, N.A., 2010. Impacts of desalination plant discharges on the marine environment: a critical review of published studies. Water Res. 44 (18), 5117-5128.

Shahmansouri, A., Min, J., Jin, L., Bellona, C., 2015. Feasibility of extracting valuable minerals from desalination concentrate: A comprehensive literature review. J. Clean. Prod. 100, 4–16.

Smičiklas, I., Dimović, S., Plećaš, I., 2007. Removal of Cs^{1+}, Sr^{2+} and Co^{2+} from aqueous solutions by adsorption on natural clinoptilolite. Appl. Clay Sci. 35, 139–144.

Smith, P., Vigneswaran, S., 2009. Effect of backwash and powder activated carbon (PAC) addition on performance of side stream membrane filtration system (SSMFS) on treatment of biological treatment effluent. Desalin. Water Treat. 11, 46–51.

U.S. Geological Survey, 2016, Mineral Commodity Summaries 2016 http://minerals.usgs.gov/minerals/pubs/mcs/index.html (accessed 20.05.17.).

Wang, Y.F., Lin, F., Pang, W.Q., 2007. Ammonium exchange in aqueous solution using Chinese natural clinoptilolite and modified zeolite. J. Hazard. Mater. 142, 160–164.

Yuan, J., Zhao, Y., Li, Q., Ji, Z., Guo, X., 2012. Preparation of potassium ionic sieve membrane and its application on extracting potash from seawater. Sep. Purif. Technol. 99, 55–60.

Supplementary Figures

Figure numbers: 4

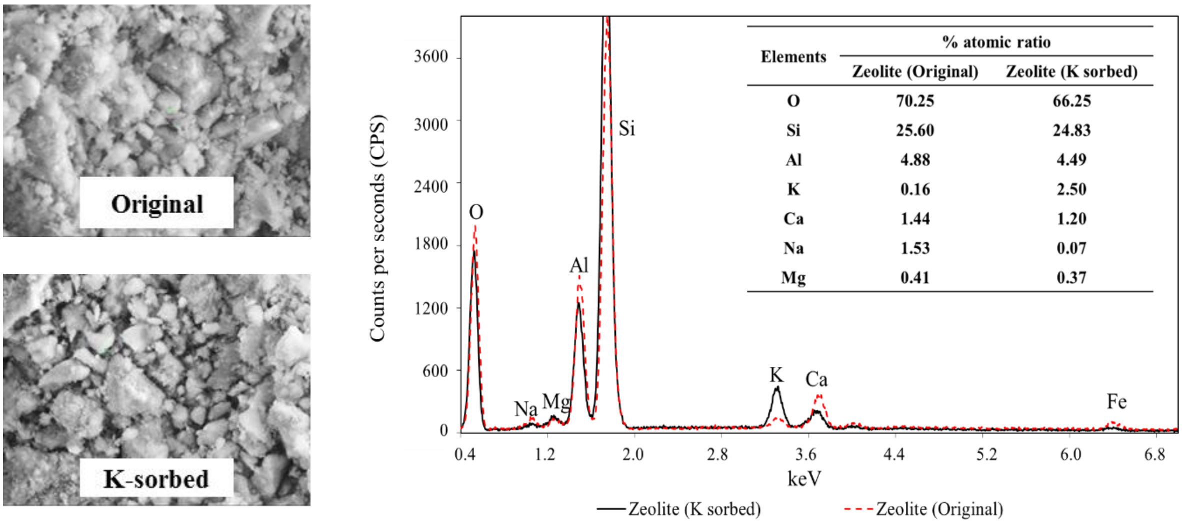

Elements	% atomic ratio	
	Zeolite (Original)	Zeolite (K sorbed)
O	70.25	66.25
Si	25.60	24.83
Al	4.88	4.49
K	0.16	2.50
Ca	1.44	1.20
Na	1.53	0.07
Mg	0.41	0.37

SEM EDX

Fig. S1. SEM–EDX analysis of original and K sorbed zeolite.

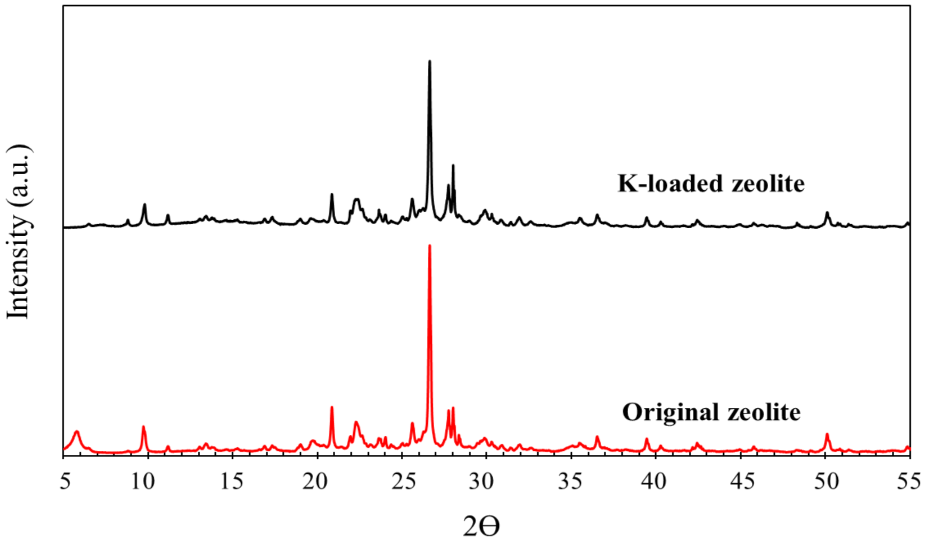

Fig. S2. XRD peaks of original zeolite and K loaded zeolite.

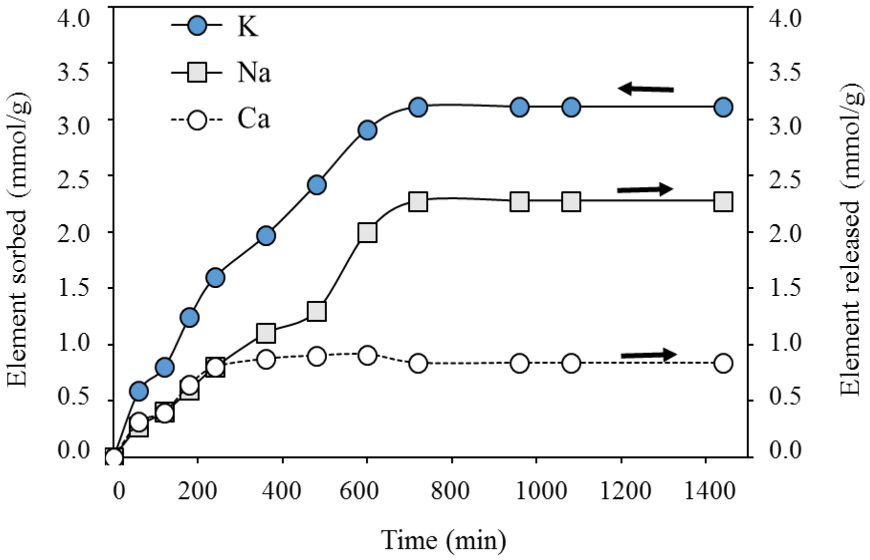

Fig. S3. Amount of K sorbed and Na and Ca released as a function of time (C_o= 790 ± 5 mg K/L; pH_{eq} = 8.0 ± 0.5; zeolite dose = 0.6 g/L) (*presented in mmol/g for element comparison*).

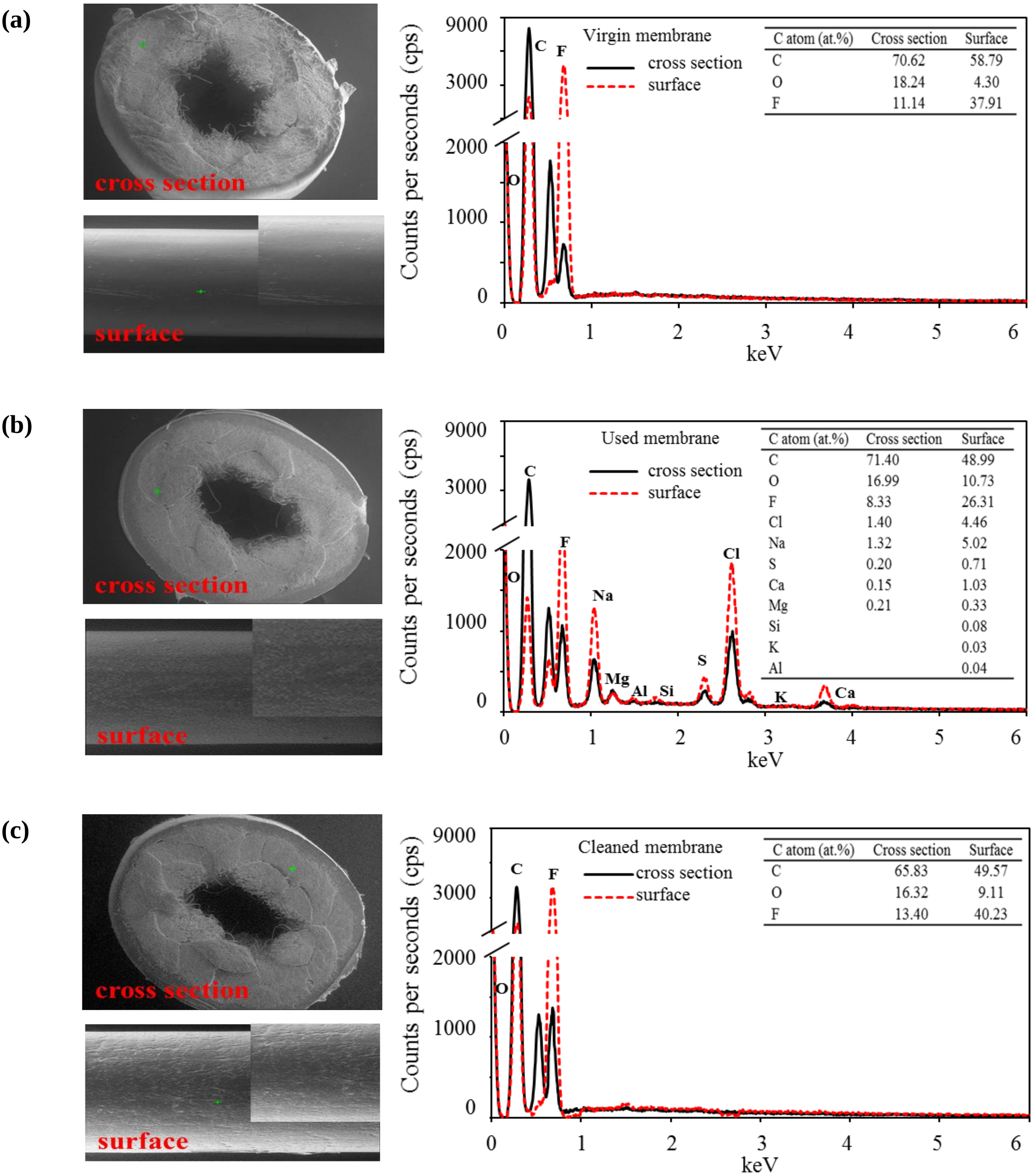

C atom (at.%)	Cross section	Surface
C	70.62	58.79
O	18.24	4.30
F	11.14	37.91

C atom (at.%)	Cross section	Surface
C	71.40	48.99
O	16.99	10.73
F	8.33	26.31
Cl	1.40	4.46
Na	1.32	5.02
S	0.20	0.71
Ca	0.15	1.03
Mg	0.21	0.33
Si		0.08
K		0.03
Al		0.04

C atom (at.%)	Cross section	Surface
C	65.83	49.57
O	16.32	9.11
F	13.40	40.23

Fig. S4. SEM-EDX analysis of surface and cross-sectioned SMSR membrane **(a)** virgin **(b)** used (tap water backwashed) **(c)** chemically cleaned.